Phys Chem Minerals (1989) 16:428–435

PHYSICS AND CHEMISTRY OF MINERALS

© Springer-Verlag 1989

Cation Disorder in Garnets Along the $Mg_3Al_2Si_3O_{12}-Mg_4Si_4O_{12}$ Join: an Infrared, Raman and NMR Study

Paul McMillan[1], Masaki Akaogi[2], Eiji Ohtani[3], Quentin Williams[4], Ronald Nieman[1], Robert Sato[1]

[1] Department of Chemistry, Arizona State University, Tempe, AZ 85287, USA
[2] Department of Earth Sciences, Kanazawa University, Kanazawa 920, Japan
[3] Department of Earth Sciences, Ehime University, Matsuyama 790, Japan
[4] Department of Geology and Geophysics, University of California, Berkeley, CA 94720*, USA

Abstract. We have obtained infrared and Raman spectra for garnets synthesized at high (static) pressures and temperatures along the join $Mg_3Al_2Si_3O_{12}$ (pyrope) – $Mg_4Si_4O_{12}$ (magnesium majorite). The vibrational spectra of Mg-majorite show a large number of additional weak peaks compared with the spectra of cubic pyrope garnet, consistent with tetragonal symmetry for the $MgSiO_3$ garnet phase. The Raman bands for this phase show no evidence for line broadening, suggesting that Mg and Si are ordered on octahedral sites in the garnet. The bands for the intermediate garnet compositions are significantly broadened compared with the end-members pyrope and Mg-majorite, indicating cation disorder in the intermediate phases. Solid state ^{27}Al NMR spectroscopy for pyrope and two intermediate compositions show that Al is present only on octahedral sites, so the cation disorder is most likely confined to Mg–Al–Si mixing on the octahedral sites. We have also obtained a Raman spectrum for a natural, shock-produced (Fe,Mg) majorite garnet. The sharp Raman peaks suggest little or no cation disorder in this sample.

Introduction

There is considerable interest in the structure and properties of high pressure phases in the system $MgO-SiO_2-Al_2O_3$ which are likely to be major components of the earth's mantle. Among these, $MgSiO_3$ with the garnet structure and its solid solutions with pyrope ($Mg_3Al_2Si_3O_{12}$) (majorites) are important both as major mineral phases of the earth's transition zone (Akaogi and Akimoto 1977; Liu 1977; Takahashi and Ito 1987; Irifune and Ringwood 1987), and because such phases are on the liquidus of ultrabasic melts at pressures between 15 and 25 GPa (Ohtani 1987). Knowledge of the physical and thermodynamic properties of these phases is important to gain a better understanding of the transition zone, and the partitioning of elements between solid and silicate liquid between 450 and 650 kilometers depth, and hence the chemical differentiation of the upper mantle (Kato et al. 1987). Majorite is moreover a transitional phase between the upper and lower mantle in a structural as well as a spatial sense, in that it contains silicon in both four- and six-fold coordination to oxygen.

The pyroxene composition $MgSiO_3$ transforms to the garnet structure above around 20 GPa and 1500° C (Kato and Kumuzawa 1985), and there is almost complete solid solution between $MgSiO_3$ and pyrope ($Mg_3Al_2Si_3O_{12}$) at lower pressures (Liu 1977; Akaogi and Akimoto 1977). Shock-produced majorite garnets containing iron are also found in some meteorites (Mason et al. 1968; Smith and Mason 1970; Jeanloz 1981). In the present study, we have obtained infrared and Raman spectra for the end-member majorite garnet ($MgSiO_3$), and for four statically-synthesized garnets in the system $Mg_3Al_2Si_3O_{12}$ (Py) – $Mg_4Si_4O_{12}$ (Mj) to investigate their structural and vibrational properties. We have also obtained solid state magic angle spinning (MAS) NMR spectra for three members of this garnet series, and have obtained the Raman spectrum for a natural, shock-produced sample of (Mg,Fe) majorite.

Experimental

The $MgSiO_3$ garnet sample was synthesized by heating at 20 GPa and 1800° C for 3 min using a multiple-anvil split-cylinder type (MA8) high pressure apparatus recently constructed at Ehime University. The sample assembly was a MgO octahedron containing a graphite sample capsule placed between two composite sheet heaters of tungsten carbide and diamond powder. Temperature was measured with a $W_{75}Re_{25}-W_{97}Re_3$ thermocouple. No pressure correction was applied to the thermocouple EMF. Further details of the furnace assembly have been described by Ohtani (1987).

The four samples Py_{100}, $Py_{82}Mj_{18}$, $Py_{59}Mj_{41}$ and $Py_{42}Mj_{58}$ (the subscript following the Mj denotes the mole per cent $Mg_4Si_4O_{12}$ component in the garnet solid solution) were synthesized at 900–1000° C at pressures between 4 and 17 GPa from glass or oxide starting mixes, and were the same samples used in the recent calorimetric and elastic studies of Akaogi et al. (1987). The natural majorite sample was obtained from R. Jeanloz, and was the same sample used in his earlier infrared and X-ray study (Jeanloz 1980).

Raman spectra were obtained on polycrystalline grains 50–100 μm in dimension using an Instruments S.A. U-1000 micro-Raman system with a Coherent Innova 90-4 argon ion laser for sample excitation. Slit widths were approximately 2 cm^{-1}, and laser power at the sample was 5–50 mW. Powder infrared spectra for the $MgSiO_3$ garnet were obtained on approximately 0.5 mg sample via the KBr disc method with a Nicolet MX-1 interferometer. Infrared

* Present address: Board of Earth Sciences, University of California, Santa Cruz, CA 95064, USA

spectra for the Py–Mj series were obtained for approximately 0.1 mg sample with a Bomem DA3.02 FTIR instrument equipped with a globar source, KBr beamsplitter and liquid-He cooled Ge:Cu detector. Solid state magic angle spinning (MAS) NMR spectra were obtained for samples of pyrope (5 mg), $Py_{82}Mj_{18}$ (2.4 mg), and $Py_{59}Mj_{41}$ (approximately 1.5 mg) using a Bruker AM-400 FT spectrometer with a Bruker MAS probe operating at 104.26 MHz for ^{27}Al. (We also attempted runs for ^{29}Si, but these were unsuccessful due to the small amounts of sample). The samples were mixed with KBr, packed into Delrin single air bearing rotors, and spun at 4.6–5.2 kHz. MAS spectra were obtained using a recycle delay of 0.5 s and a 60° pulse (90° = 3.8 μs). The magic angle was detuned 1–2° to reduce spinning side bands (Oldfield et al. 1982). Chemical shifts are reported in ppm relative to $Al(H_2O)_6^{3+}$ (1M $AlCl_3$ in H_2O).

Results and Discussion

Pyrope

Pyrope has a cubic garnet structure with space group Ia3d (Oh^{10}) and four formula units ($Mg_3Al_2Si_3O_{12}$) per primitive cell. Moore et al. (1971) have carried out a symmetry analysis for the cubic garnet structure to determine the expected optically active vibrations:

Raman: $3A_{1g}+8E_g+14T_{2g}$
Infrared: $17T_{1u}$
Inactive: $5A_{2g}+14T_{1g}+5A_{1u}+5A_{2u}+10E_u+16T_{2u}$.

The Raman spectrum of pyrope shows ten prominent peaks, and a further three to five peaks may be distinguished as shoulders or weak features in the spectrum (Fig. 1; Table 1). Moore et al. (1971) obtained polarized Raman spectra for a grossularite ($Gr_{90}Al_3An_6$), and found the three A_{1g} modes at 888, 557 and 378 cm^{-1}. Several authors (Tarte 1965; Moore et al. 1971; Tarte and Deliens 1973) have demonstrated a general decrease in frequency of the infrared and Raman bands of silicate garnets with increasing cell edge, especially for peaks above 500 cm^{-1}. Pyrope has a smaller cell volume than grossular, and it seems reasonable to assign the three prominent Raman peaks of pyrope at 928, 562 and 364 cm^{-1} to the expected

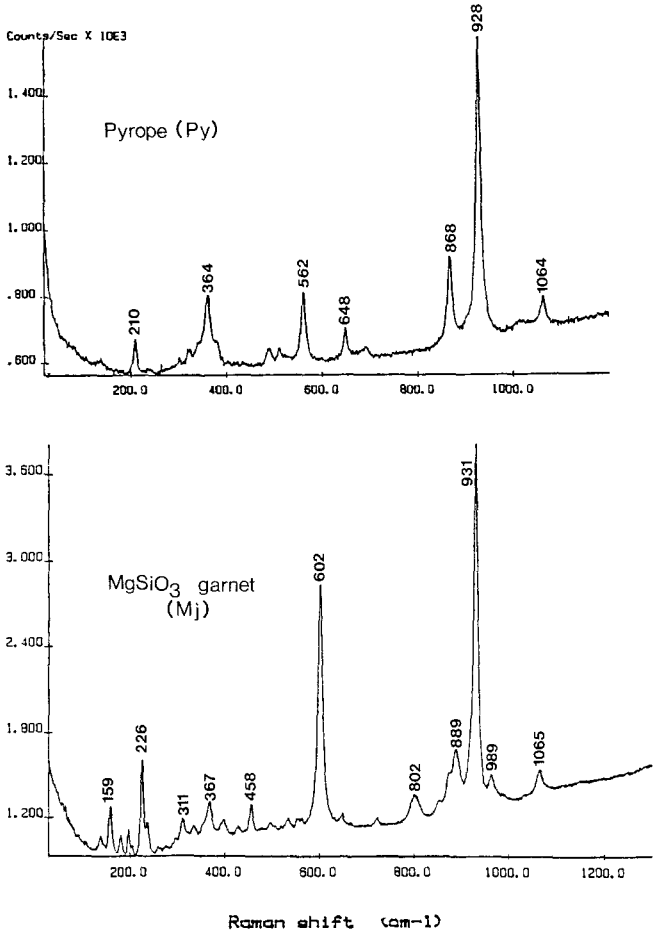

Fig. 1. Raman spectra of pyrope (Py) and $MgSiO_3$ garnet (Mj)

Table 1. Infrared and Raman peak positions for pyrope and $MgSiO_3$ garnet. w – weak; s – strong; sh – shoulder. For infrared data: (a) Kato and Kumazawa (1985); (b) this study (Figure 2)

Raman		Infrared		
Pyrope	$MgSiO_3$ garnet	Pyrope	$MgSiO_3$ garnet	
			(a)	(b)
	138			
	159			
	181			
210	197, 205			
218 sh	226, 238 sh			
	261			
	275			
	293			
320	311			
340 sh	336	340		354
364	354, 367			362 sh?
382 sh				383
	398	390	395	398
				416 w,sh
	429			433 sh
			442	446
	458	466	458	459
	481	485		490
492	498			
512	507		501	501 sh
			520	521
	535	538	549	549
	559	584	576	580
562	602 s	615 sh		604 sh
			627	632
648	648			
656 sh?			670	675
			693	693 w
	724			
	802 w			
			831	827 s
868	852, 873 sh	877	876	879
910 sh	889	907	903	906
928 s	931 s			
	964	976	950	954
	989			
		1003 sh	998	1002
	1034			
1064 w	1065			

A_{1g} modes. Also by analogy with the Gr_{90} spectrum of Moore et al. (1971), it is likely that the 868 cm^{-1} peak of pyrope is of E_g symmetry.

The tetrahedral SiO_4 groups in the cubic garnet structure occupy sites with S_4 symmetry. By analogy with other orthosilicates, the Si–O stretching vibrations of these should lie above 800 cm^{-1}. The ν_1 symmetric stretching vibrations give rise to two Raman modes ($A_{1g}+E_g$), while the ν_3 asymmetric stretching vibrations give rise to four Raman modes of the crystal, E_g+3T_{2g} (Moore et al. 1971). Since the A_{1g} and E_g vibrations are associated with diagonal elements of the Raman scattering tensor (α_{xx}, α_{yy} and α_{zz}), they should give rise to more intense bands than the T_{2g} modes which are associated only with off-diagonal elements, while the more symmetric ν_1-derived vibrations should give stronger Raman peaks than those derived from the asymmetric stretch. From this, is likely then that the 928 and 868 cm^{-1} peaks of pyrope correspond to the A_{1g} and E_g modes derived from ν_1, while the peak at 1064 cm^{-1}, the shoulder at 910 cm^{-1}, and perhaps the weak feature visible near 1010 cm^{-1} correspond to the E_g and T_{2g} modes derived from ν_3. The A_{1g} mode at 562 cm^{-1} is derived from the ν_2 symmetric bending vibration of the SiO_4 groups, while the lowest frequency A_{1g} vibration can be assigned to a rotatory motion of the silicate tetrahedra (Moore et al. 1973). The peaks in the Raman spectrum of pyrope are all sharp, with comparable half-widths to those of forsterite (10–15 cm^{-1}: Piriou and McMillan 1983). This suggests that the pyrope garnet is well ordered,consistent with previous single crystal refinements, which indicate all Si ordered on tetrahedral sites, and all Al on octahedral sites (Gibbs and Smith 1965; Meagher 1975; Hazen and Finger 1978; Levien et al. 1979). As part of this study, we obtained a ^{27}Al MAS NMR spectrum for pyrope (Fig. 5). This showed only a single peak at 2.8 ppm, again consistent with all Al ordered on octahedral sites in the garnet (Muller et al. 1981).

The infrared spectrum of pyrope (Fig. 2; Table 1) is similar to that obtained by Tarte (1965). The weak bands near 1088 and 1160 cm^{-1} were not observed by Tarte (1965) (although similar bands appear in the spectrum of Cahay et al. 1981), and probably correspond to a trace of unreacted silica in the sample (also the weak feature near 800 cm^{-1}). No corresponding features were observed in the Raman spectrum.

As noted above, factor group analysis predicts 17 infrared bands of T_{1u} symmetry. Of these, three should be derived from the ν_3 asymmetric stretching vibrations of the SiO_4 tetrahedra, and none from the ν_1 symmetric stretch (Moore et al. 1971). The observed infrared spectrum of pyrope contains *four* features in the Si–O stretching region: bands at 976, 907 and 877 cm^{-1}, and a shoulder at 1003 cm^{-1}. These correspond respectively to bands B, C, D and A of Tarte (1965), Tarte and Deliens (1973), and Moore et al. (1971), and are observed in the powder infrared spectra of a wide variety of silicate garnets (Omori 1971; Moore et al. 1971; Nishizawa and Koizumi 1975; Tarte et al. 1979) and yttrium aluminium garnet (Slack et al. 1969; McDevitt 1969). The increased number of bands could indicate a lower symmetry than S_4 for the SiO_4 groups in pyrope, or a distortion of the garnet from cubic symmetry. Although such distortions are known for some garnets (Ringwood and Major 1967; Prewitt and Sleight 1969; Akimoto and Syono 1972; Kato and Kumazawa

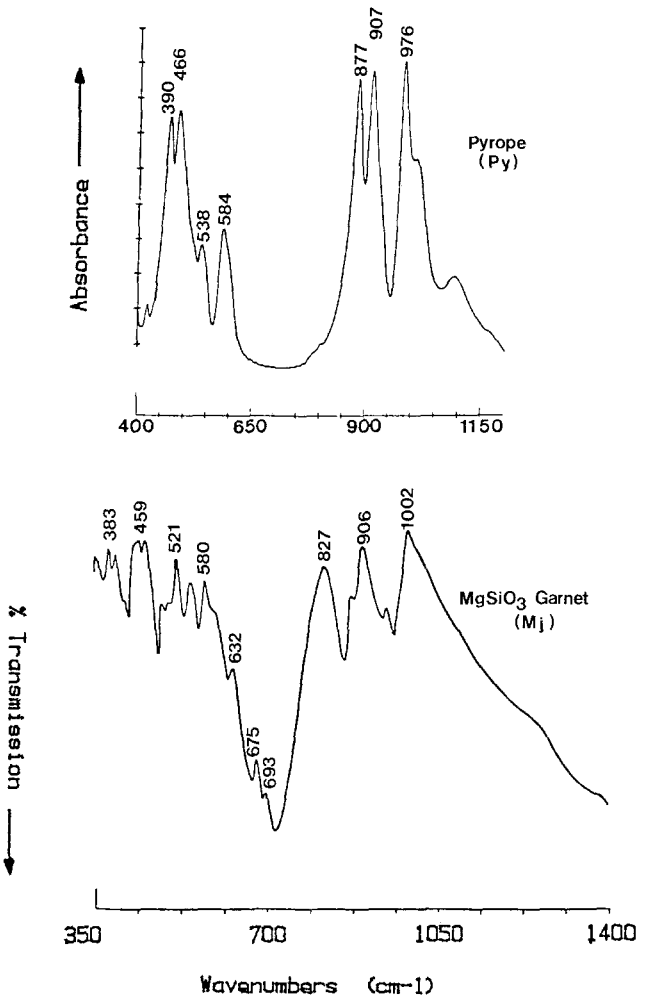

Fig. 2. Infrared transmission spectra of pyrope (Py) and $MgSiO_3$ garnet (Mj). Note that the infrared spectrum of pyrope is plotted in absorbance units. The weak bands near 1088 and 1160 cm^{-1} in the pyrope spectrum are due to a trace of silica impurity, as discussed in the text

1985; Fujino et al. 1986; Allen and Buseck 1988), the single crystal X-ray data for pyrope show no evidence of lower symmetry than cubic for pyrope (Gibbs and Smith 1965; Meagher 1975; Hazen and Finger 1978; Levien et al. 1979), while our ^{27}Al NMR data show only a single peak for octahedral Al (Fig. 5), indicating no cation site disorder in the garnet. The origin of the high frequency shoulder (1003 cm^{-1}) in the infrared spectrum of pyrope is not yet clear. From infrared spectra of silicate impurities in aluminate garnets, it is unlikely that this band corresponds to a fundamental transverse optic mode of the lattice (Wickersheim et al. 1960). The isotopic substitution data of Cahay et al. (1981) show that it is associated with motion of the silicon (tetrahedral) cation. Suwa and Naka (1975) and Cahay et al. (1981) attribute the band to a combination mode, perhaps between an internal vibration of the SiO_4 unit and an external (lattice) vibration. A second possibility is that this band corresponds to a longitudinal optic component associated with one of the ν_3 bands, due to a component of reflection being present in the powder transmission spectra. Resolution of this problem will require single crystal infrared reflectance studies for pyrope, and the other garnets affected.

$MgSiO_3$ Garnet

Kato and Kumazawa (1985) have suggested that $MgSiO_3$ garnet has tetragonal symmetry, based on small splittings in its X-ray diffraction pattern and from the form of its infrared spectrum. The Raman and infrared spectra of $MgSiO_3$ garnet are shown in Figures 1 and 2, compared with those for pyrope. Peak positions are listed in Table 1. Our infrared spectrum is similar to that of Kato and Kumazawa (1985), but more peaks are visible in the present spectrum. The Raman spectra for pyrope and $MgSiO_3$ garnet are quite similar, except that many more peaks are apparent for the $MgSiO_3$ sample.

Fujino et al. (1986) found space group $I4_1/a$ (corresponding to point group C_{4h}) for the tetragonal garnet $MnSiO_3$. A similar tetragonal distortion from the cubic space group Ia3D (O_h) for $MgSiO_3$ would most likely give a phase with the same symmetry, or perhaps a higher symmetry phase with factor group D_{4h}. From correlation of symmetry species between point groups O_h, D_{4h} and C_{4h}, we can predict the number and activities of the vibrational modes for these tetragonal garnet structures. For a tetragonal D_{4h} structure, we expect

$$11A_{1g}(R)+14A_{2g}+13B_{1g}(R)+14B_{2g}(R)+28E_g(R)+15A_{1u}+17A_{2u}(IR)+15B_{1u}+16B_{2u}+33E_u(IR)$$

(R) and IR indicate Raman and infrared activity), while for a tetragonal C_{4h} structure, we expect

$$25Ag(R)+27B_g(R)+28E_g(R)+32A_u(IR)+31B_u+33E_u(IR).$$

It is obvious that tetragonal distortion of the garnet structure results in many more Raman and infrared active peaks, consistent with the observed spectra of $MgSiO_3$ garnet compared with pyrope. This supports Kato and Kumazawa's (1985) suggestion that $MgSiO_3$ garnet has tetragonal symmetry. We can investigate this further by considering the high frequency region of the infrared and Raman spectra of both phases.

The peaks above 800 cm^{-1} in the vibrational spectra of orthosilicates can often be usefully assigned to stretching vibrations of the SiO_4 tetrahedral groups (Piriou and McMillan 1983). For a cubic (O_h) garnet structure, we expect the ν_1 and ν_3 symmetric and asymmetric stretching vibrations of the SiO_4 groups to give rise to the following Raman and infrared active modes (Moore et al. 1971):

$$\nu_1 \text{-----} A_{1g}(R)+E_g(R)$$
$$\nu_3 \text{-----} E_g(R)+3T_{2g}(R)+3T_{1u}(IR).$$

As discussed above, the A_{1g} mode is likely responsible for the strong Raman line at 928 cm^{-1} for pyrope, while the modes at 868 and 1064 cm^{-1} are probably of E_g symmetry, derived from ν_1 and ν_3 vibrations respectively. Other weak features in the high frequency Raman spectrum are due to the T_{2g} modes derived from ν_3. On distortion to a tetragonal D_{4h} structure, the SiO_4 stretching vibrations would give rise to the following infrared and Raman active modes:

$$\nu_1: 2A_{1g}(R)B_{1g}(R)+E_g(R)+E_u(IR)$$
$$\nu_3: A_{1g}(R)+2B_{1g}(R)+3B_{2g}(R)+5E_g(R)+3A_{2u}(IR)+5E_u(IR).$$

The Raman spectrum of $MgSiO_3$ garnet shows eight obvious high frequency modes compared to the fifteen expected for a D_{4h} structure (Fig. 1). The strong Raman mode at 931 cm^{-1} is likely the A_{1g} mode derived from the ν_1 symmetric stretch, and the 1065 cm^{-1} band probably corresponds to one of the E_g modes derived from ν_3, as for pyrope. The other high frequency peaks cannot be easily assigned. The high frequency infrared spectrum of $MgSiO_3$ garnet shows three strong bands at 827, 906 and 1002 cm^{-1}, which probably correspond to the three modes expected for a cubic structure, and two additional weak peaks at 954 and 879 cm^{-1}. If the factor group were C_{4h} rather than D_{4h}, as found for $MnSiO_3$ garnet by Fujino et al. (1986), even more peaks would be present in the infrared and Raman spectra, so that it is not necessary to invoke the lower point symmetry to interpret the observed spectra of $MgSiO_3$ garnet (although this is not a conclusive argument for the higher symmetry tetragonal point group, and a careful diffraction study will be required to determine the true structure).

There is a prominent peak at 602 cm^{-1} in the Raman spectrum of $MgSiO_3$ garnet. This is a region commonly assigned to vibrations of SiOSi linkages in condensed silicates (McMillan 1984). As noted above, there is a peak in the 500–600 cm^{-1} region of grossular and pyrope, assigned to an A_{1g} mode derived from OSiO bending of the tetrahedral SiO_4 groups. In the case of $MgSiO_3$ garnet, the tetrahedral SiO_4 units share corners with octahedral SiO_6 groups, so such OSiO bending vibrations would also be described as SiOSi linkage vibrations. We suggest that this might be a good description for the peak at 602 cm^{-1} in the spectrum of $MgSiO_3$ garnet.

We observe weak peaks at 693 and 670 cm^{-1} in the infrared spectrum of $MgSiO_3$ garnet, which are not present in the spectrum of pyrope (Fig. 2). These weak bands appear gradually with increasing $MgSiO_3$ content in the pyrope-majorite garnet series discussed below. Jeanloz (1980) suggested that a similar weak peak in the infrared spectrum of Fe-rich natural majorite could be due to a vibration of octahedral SiO_6 groups in the structure. If so, these would be more likely due to deformation fibrations of the SiO_6 groups rather than Si–O stretching (Williams et al. 1987). Although this could be a useful interpretation of the bands in the infrared spectra, the Raman spectrum of pyrope, which contains no SiO_6 units, also shows weak peaks in this same region.

Two of the most interesting features of the $MgSiO_3$ spectra are (a) that the observed peak positions are very similar to those of pyrope (except for additional bands due to the lower symmetry), and (b) that the peak widths in both phases are similar. The first observation suggests that the vibrational spectra are little affected by replacing 2Al by Mg+Si within the garnet structure, and the second suggests that both pyrope and $MgSiO_3$ garnet have similar degrees of cation order. Since previous X-ray studies and our present ^{27}Al NMR results indicate an ordered structure for pyrope, we suggest that $MgSiO_3$ garnet is also perfectly ordered, with Mg on dodecahedral sites, Mg+Si ordered on octahedral sites, and Si on tetrahedral sites. Both observations together suggest that there should be little difference in vibrational or configurational entropy between the end-member pyrope and $MgSiO_3$ garnets.

Garnets in the $Mg_3Al_2Si_3O_{12}$ – $Mg_4Si_4O_{12}$ Series

The infrared and Raman spectra of four garnets in the $Mg_3Al_2Si_3O_{12}$ – $Mg_4Si_4O_{12}$ (Py–Mj) solid solution series

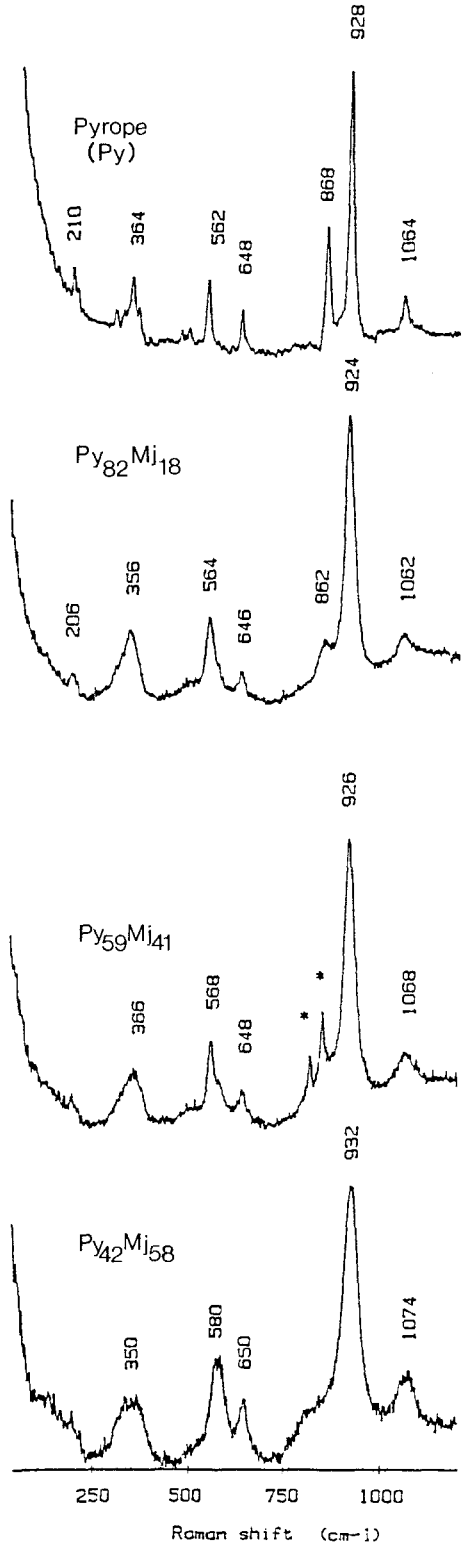

Fig. 3. Raman spectra of garnets along the $Mg_3Al_2Si_3O_{12}$ (Py)–$Mg_4Si_4O_{12}$ (Mj) join

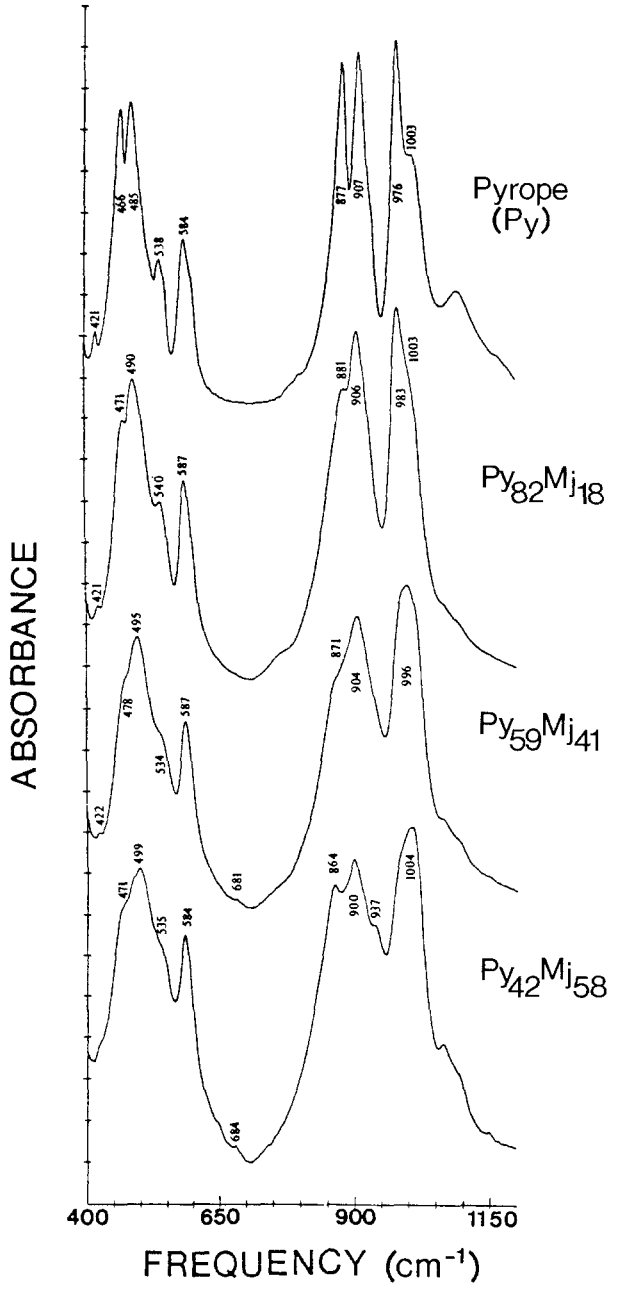

Fig. 4. Infrared spectra of garnets along the $Mg_3Al_2Si_3O_{12}$ (Py) – $Mg_4Si_4O_{12}$ (Mj) join

are shown in Figures 3 and 4. The weak sharp Raman peaks at 826 and 858 cm^{-1} observed for the $Py_{59}Mj_{41}$ composition correspond to a trace of forsterite impurity, not observed by X-ray or optical examination. Pure pyrope garnet contains Si on tetrahedral sites, Al on octahedral sites, and Mg in eight-fold coordination to oxygen. Addition of $MgSiO_3$ component formally replaces aluminium in the pyrope structure by silicon and magnesium. The garnets in the Py–Mj series studied all have much broader Raman bands (FWHM = 40–50 cm^{-1}) than pyrope. Such line broadening is generally associated with structural disorder over lattice sites. Since the crystal chemical substitution in the Py–Mj garnet series is formally Mg + Si = 2Al on octahedral aluminium sites, the band broadening could be associated with simply Mg, Si and Al disorder over octahedral sites in intermediate garnets, but there could also be disorder on tetrahedral and/or dodecahedral sites. In order to partly resolve this question, we obtained ^{27}Al MAS NMR spectra for two samples in the Py–Mj series ($Py_{59}Mj_{41}$ and $Py_{59}Mj_{41}$). The NMR spectra (Fig. 5) show a single strong peak near 2 ppm (there is a small shift to

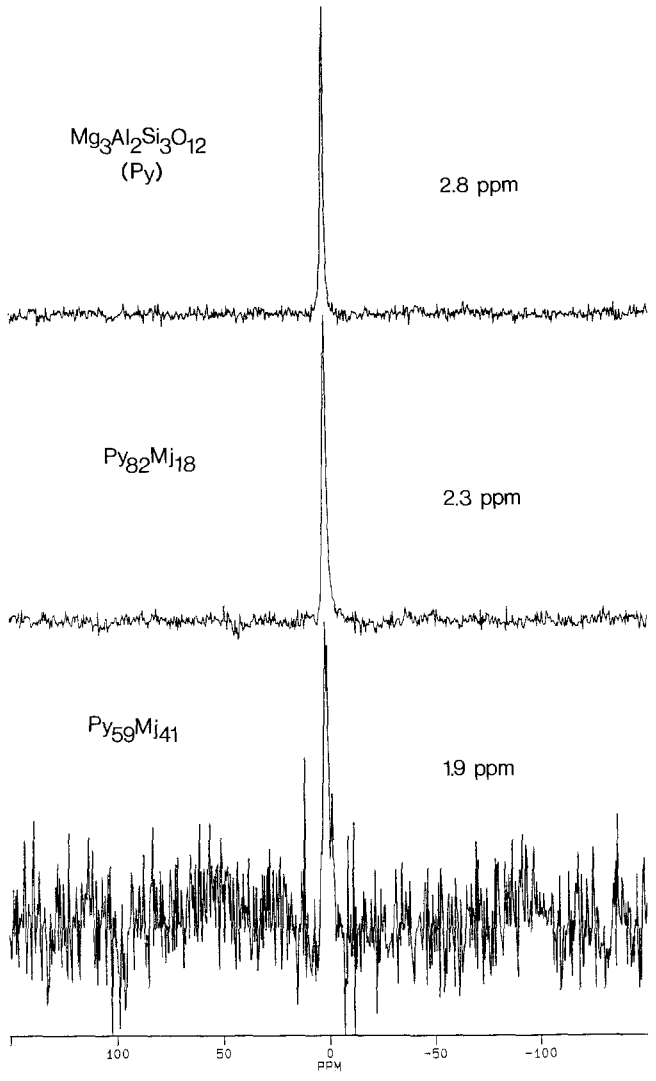

Fig. 5. ^{27}Al MAS NMR spectrum of pyrope (Py) and the intermediate garnets $Py_{82}Mj_{18}$ and $Py_{59}Mj_{41}$

lower ppm values with increasing Mj content), consistent with only octahedral (i.e., no dodecahedral or tetrahedral) aluminium in these garnets (Muller et al. 1981). This result strongly suggests that cation disorder is confined to Mg–Si–Al mixing on the octahedral sites within the $Mg_3Al_2Si_3O_{12}$ – $Mg_4Si_4O_{12}$ garnet series. This type of disorder was assumed by Akaogi et al. (1987) along with thermochemical data to calculate phase relations within the system $Mg_4Si_4O_{12}$–$Mg_3Al_2Si_3O_{12}$ at mantle pressures and temperatures. These workers also assumed that no cation disorder was present in end-member Mg-majorite. Our results suggest that both of these assumptions were valid, and that the phase diagrams proposed by Akaogi et al. (1987) are essentially correct.

There is remarkably little shift in the vibrational frequencies with composition within this garnet series, suggesting that the Mg+Si=2Al substitution has little effect on the garnet force field. This in striking contrast to the observed spectral differences between Al_2O_3 corundum and $MgSiO_3$ ilmenite (McMillan and Ross 1987). This invariance in peak positions for the garnets suggests that the substitution has little effect on the vibrational entropy, and that any entropy of mixing arises from the configurational terms.

There are some small systematic changes in the infrared spectra which can be understood on crystal chemical grounds. Moore et al. (1971) have suggested that the separation of bands C and D (907 and 877 cm^{-1} for pyrope), or site group splitting, is indicative of the degree of distortion of the SiO_4 groups in the garnet. Despite the observed band broadening, the site group splitting remains nearly constant across the series at 30–35 cm^{-1}, showing that the distortion of the SiO_4 groups is unchanged. Novak and Gibbs (1971) have shown that the tetrahedral Si–O bond length in silicate garnets is insensitive to the nature of either the octahedral or dodecahedral cations, as long as the mean radius of the dodecahedral cation is less than 1 Å, which would be the case for Mg^{2+} (or Fe^{2+} in Fe-majorites). On the other hand, the angular distortion of the SiO_4 unit is dominantly dependent on the nature of the dodecahedral cation. However, this is likely to remain Mg^{2+} throughout the present series, as discussed above. Both arguments are consistent with the observed constant site group splitting within the present Py–Mj garnet series. For comparison, Jeanloz (1981) found a site group splitting of 55 cm^{-1} for a natural meteoritic majorite sample $Mg_{0.79}Fe_{0.21})SiO_3$, which suggests that iron substitution in the dodecahedral site has a large effect on distortion of the SiO_4 group. We cannot simply estimate the site group splitting for the Mg-majorite end member, due to the extra peaks appearing associated with the lowered symmetry (Fig. 2; Table 1).

Moore et al. (1971) also defined a factor group splitting for silicate garnets, defined as the frequency ratio of infrared bands (B–(C+D)/2) (bands B, C and D for pyrope occur at 976, 907 and 877 cm^{-1} respectively), which indicates the degree of vibrational interaction between SiO_4 groups within the unit cell. In contrast to the small change in site group splitting observed for the Py–Mj garnets, the factor group splitting increases from 84 cm^{-1} for pyrope to 122 cm^{-1} for the composition $Py_{42}Mj_{58}$ (bands B, C and D identified at 1004, 900 and 864 cm^{-1} respectively). This is the largest factor group splitting yet reported for any garnet, and indicates a strong vibrational coupling between SiO_4 groups. This is probably associated with the formation of strong SiOSi linkages between tetrahedral and octahedral silicate units as Mg+Si is substituted for 2Al on octahedral sites, and is consistent with our interpretation of the strong 602 cm^{-1} Raman band of $MgSiO_3$ garnet as an SiOSi linkage vibration.

Natural Shock-Produced (Fe,Mg) Majorite

Finally, in Figure 6 we show the Raman spectrum of a natural majorite sample $(Mg_{0.79}Fe_{0.21})SiO_3$, extracted by Jeanloz (1980) from a thin section of the Catherwood meteorite (Coleman 1977). The Raman spectrum is similar to that of pyrope. The principal Si–O stretching peak remains at the same frequency (928–929 cm^{-1}), while the 868 cm^{-1} peak of pyrope has probably shifted to become the shoulder in the majorite spectrum near 900 cm^{-1}. The two modes of pyrope at 562 and 648 cm^{-1} have also incresed in frequency, to become the 592 and 700 cm^{-1} peaks of majorite. The 562 cm^{-1} band of pyrope is derived from an OSiO bending vibration of the SiO_4 tetrahedra. The increase in frequency with increasing majorite content may reflect an increased stiffening in the net OSiO bending force constant as Si is substituted for Al in the octahedral site. Although it is difficult to tell with the broad background in the major-

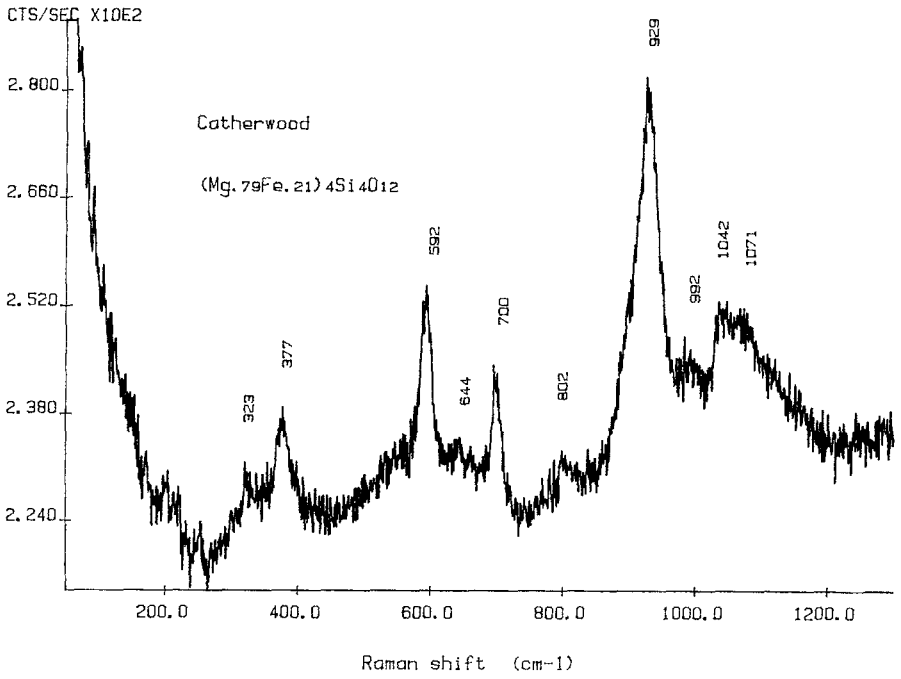

Fig. 6. Raman spectrum of a natural sample of (Fe,Mg) majorite garnet from Catherwood meteorite

ite spectrum, we find no evidence for extra weak peaks or mode splitting suggesting a deviation from cubic symmetry. This is consistent with the X-ray and infrared study of Jeanloz (1980) on the same sample. The broad weak background features could form part of the natural majorite spectrum, which would indicate some disorder or strain in the structure, or could be due to some diaplectic glass mixed in with the majorite (Price et al. 1979; Jeanloz 1980). The peaks for this natural majorite are visibly narrower than those for intermediate garnets in the Py–Mj series, suggesting a greater degree of order on the cation sites. In the present study, we have suggested that Mg and Si may be ordered within the octahedral sites of $MgSiO_3$ garnet. It is possible that within the natural majorite, Fe and Mg are ordered on dodecahedral sites, and (Fe,Mg,Si) are ordered within the octahedral sites. However, this would result in peak splitting in the infrared and Raman spectra, since the SiO_4 sites would have lower than S_4 symmetry. No such splitting was detected at the present resolution. More work will be needed to characterize the cation site distributions of Fe-containing majorites, both for samples prepared via high temperature-high pressure synthesis relevant to mantle phase equilibria, and samples produced by shock.

Acknowledgements. P. McMillan and R. Sato were supported by NSF grant EAR-8616990, Q. Williams by NSF grant EAR-860461 at U.C. Berkeley, and M. Akaogi by grants 60840023 and 62540618 from the Ministry of Education, Science and Culture, Japan. M. Akaogi thanks S. Akimoto for the use of his facilities in the synthesis of the pyrope and intermediate garnet samples. The NMR spectrometer was purchased with funds from Arizona State University and the National Science Foundation (CHE-8409644). We thank both reviewers for their constructive comments.

References

Akaogi M, Akimoto S (1977) Pyroxene-garnet solid solution equilibria in the systems $Mg_4Si_4O_{12}-Mg_3Al_2Si_3O_{12}$ and $Fe_4Si_4O_{12}-Fe_3Al_2Si_3O_{12}$ at high pressures and temperatures. Phys Earth Planet Interiors 15:90–106

Akaogi M, Navrotsky A, Yagi T, Akimoto S-I (1987) Pyroxene-garnet transformations: thermochemistry and elasticity of garnet solid solutions, and application to a pyrolite mantle. In: High-Pressure Research in Mineral Physics, Manghnani MH, Syono Y (eds), pp 251–260, Am Geophys Union

Akimoto S-I, Syono Y (1972) High pressure transformations in $MnSiO_3$. Am Mineral 57:76–84

Allen FM, Buseck PR (1988) An XRD, FTIR and TEM study of optically anisotropic grossular garnets. Am Mineral, in press

Cahay R, Tarte P, Fransolet AM (1981) Interprétation du spectre infrarouge de variétés isotopiques de pyropes synthétiques. Bull Minéral 104:193–200

Fujino K, Momoi H, Sawamoto H, Kumazawa M (1986) Crystal structure and chemistry of $MnSiO_3$ tetragonal garnet. Am Mineral 71:781–785

Gibbs GV, Smith JV (1965) Refinement of the crystal structure of pyrope. Am Mineral 50:2023–2039

Hazen RM, Finger LW (1978) Crystal structures and compressibilities of pyrope and grossular to 60 kbar. Am Mineral 63:297–303

Irifune T, Ringwood AE (1987) Phase transformations in primitive MORB and pyrolite compositions to 25 GPa and some geophysical implications. In: High-Pressure Research in Mineral Physics, Manghnani MH, Syono Y (ed), pp 231–242, Am Geophys Union

Jeanloz R (1980) Majorite: vibrational and compressional properties of a high-pressure phase. J Geophys Res 86B:6171–6179

Kato T, Kumazawa M (1985) Garnet phase of $MgSiO_3$ filling the pyroxene-ilmenite gap at very high temperature. Nature 316:803–804

Kato T, Irifune T, Ringwood AE (1987) Majorite partition behavior and petrogenesis of the Earth's upper mantle. Geophys Res Lett 14:546–549

Levien L, Prewitt CT, Weidner DJ (1979) Compression of pyrope. Am Mineral 64:805–808

Liu LG (1977) The system enstatite-pyrope at high pressures and temperatures and the earth's mantle. Earth Planet Sci Letts 36:237–245

Mason B, Nelen J, White JS Jr (1968) Olivine-garnet transformation in a meteorite. Science 160:66–67

McDevitt NT (1969) Infrared lattice spectra of rare-earth aluminium, gallium and iron garnets. J Opt Soc Am 59:1240–1244

McMillan P (1984) Structural studies of silicate glasses and melts:

applications and limitations of Raman spectroscopy. Am Mineral 69:622–644

McMillan P, Ross N (1987) Heat capacity calculations for Al_2O_3 corundum and $MgSiO_3$ ilmenite. Phys Chem Minerals 14:225–234

Meagher EP (1975) The crystal structures of pyrope and grossularite at elevated temperatures. Am Mineral 60:218–228

Moore RK, White WB (1971) Vibrational spectra of the common silicates: I. The garnets. Am Mineral 56:54–71

Muller D, Gessner W, Behrens HJ, Scheler G (1981) Determination of the aluminium coordination in aluminium-oxygen compounds by solid-state high-resolution ^{27}Al NMR. Chem Phys Lett 79:59–62

Nishizawa H, Koizumi M (1975) Synthesis and infrared spectra of $Ca_3Mn_2Si_3O_{12}$ and $Cd_3B_2Si_3O_{12}$ (B:Al,Ga,Cr,V,Fe,Mn) garnets. Am Mineral 60:84–87

Novak GA, Gibbs GV (1971) The crystal chemistry of the silicate garnets. Am Mineral 56:791–825

Ohtani E (1987) Ultrahigh-pressure melting of a model chondritic mantle and pyrolite compositions. In: High-Pressuer Research in Mineral Physics, ed Manghnani MH, Syono Y, pp 87–93. Am Geophys Union

Oldfield E, Kinsey RA, Montez B, Ray T, Smith KA (1982) High-resolution solid-state NMR spectra of quadrupolar nuclei: Magic angle and off-axis spinning of vanadium-51 (I = 7/2) in sodium and ammonium vanadates. J Chem Soc: Chem Comm 254–256

Omori K (1971) Analysis of the infrared absorption spectrum of almandine-pyrope garnet from Nijosan, Osaka Prefecture, Japan. Am Mineral 56:841–849

Piriou B, McMillan P (1983) The high frequency vibrational spectra of crystalline and vitreous orthosilicates. Am Mineral 68:426–443

Price GD, Putnis A, Agrell SO (1979) Electron petrography of shock-produced veins in the Tenham chondrite. Contrib Mineral Petrol 18:175–198

Slack GA, Oliver DW, Chrenko RM, Roberts S (1969) Optical absorption of $Y_3Al_5O_{12}$ from 10- to 55000 wavenumbers. Phys Rev 177:1308–1314

Smith JV, Mason B (1970) Pyroxene-garnet transformation in Coorara meteorite. Science 168:832–833

Suwa Y, Naka S (1975) Infrared spectra of the solid solution between uvarovite and spessartine. Am Mineral 60:1125–1126

Takahashi E, Ito E (1987) Ultrahigh-pressure phase transformations and the composition of the deep mantle. In: High-Pressure Research in Mineral Physics, Manghnani MH, Syono Y, (Ed), pp 221–229, Am Geophys Union

Tarte P (1965) Etude expérimentale et interprétation du spectre infra-rouge des silicates et germanates. Application à des problèmes structuraux relatifs à l'état solide. Mémoires de l'Académie Royale de Belgique 35. Parts 4(a) and 4(b); 259 pp and 134 pp

Tarte P, Deliens M (1973) Correlations between the infrared spectrum and the composition of garnets in the pyrope-almandine-spessartine series. Contrib Mineral Petrol 40:25–37

Tarte P, Cahay R, Garcia A (1979) Infrared spectrum and structural role of titanium in synthetic Ti-garnets. Phys Chem Minerals 4:55–63

White WB, Keramidas V (1971) Raman spectra of yttrium iron garnet and two vanadium garnets. J Am Ceram Soc 54:472–473

Wickersheim KA, LeFever RA, Hanking BM (1960) Infrared absorption of the silicate ion in the garnet structure. J Chem Phys 22:271–276

Williams Q, Jeanloz R, McMillan P (1987) Vibrational spectra of $MgSiO_3$-perovskite: zero pressure Raman and mid-infrared spectra to 27 GPa. J Geophys Res 92:8116–8128

Received June 28, 1988